Structural Optimization **10**, 40–45 © Springer-Verlag 1995

Checkerboard patterns in layout optimization

A. Díaz

Department of Mechanical Engineering, Michigan State University, East Lansing, MI 48824, USA

O. Sigmund

Department of Solid Mechanics, Technical University of Denmark, DK-2800 Lyngby, Denmark

Abstract Effective properties of arrangements of strong and weak materials in a checkerboard fashion are computed. Kinematic constraints are imposed so that the displacements are consistent with typical finite element approximations. It is shown that when four-node quatrilateral elements are involved, these constraints result in a numerically induced, artificially high stiffness. This can account for the formation of checkerboard patterns in continuous layout optimization problems of compliance minimization.

1 Introduction

The popularity of layout optimization methods in structural design has increased rapidly since the publication of the paper by Bendsøe and Kikuchi (1988) triggered a renewed interest in the topic. Since then several different versions of the problem have been developed and a fair amount of debate has taken place in the literature and at specialized meetings regarding the advantages and disadvantages of the different approaches. However, while there are indeed fundamental differences that distinguish the more popular methods in use today, experiments have shown that most methods have in common one undesirable feature: they may result in solutions where material is distributed in a *checkerboard pattern*. In layout problems where the amount of material present at a location x is measured by the scalar *density* function $\rho(x)$, a checkerboard pattern is defined as a periodic pattern of high and low values of $\rho(x)$ arranged in the fashion of a checkerboard, as illustrated in Fig. 1. This behaviour is *undesirable* as it is the result of a numerical instability and does not correspond to an optimal distribution of material. In this paper we discuss the reasons for the formation of such patterns.

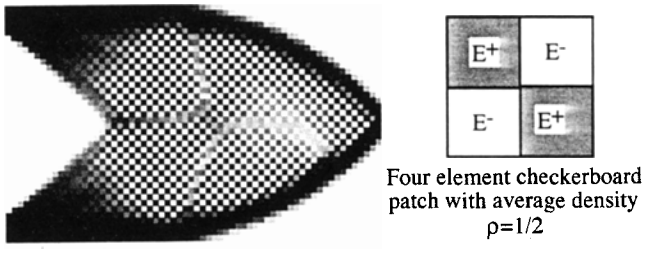

Fig. 1. Solution displaying checkerboard patterns

The literature offers only little discussion on the formation of checkerboards in layout optimization problems (Bendsøe *et al.* 1992; Jog *et al.* 1992; Bendsøe 1994; Jog and Haber 1994), although similar patterns affecting the finite element solution of mixed variational problems have been studied extensively (see e.g. Brezzi and Fortin 1991). In such problems the formation of checkerboards is related to the violation of the so-called Babuska-Brezzi or LBB condition. This similarity was used by Jog *et al.* (1992) and Jog and Haber (1994) to attribute the patterns in the layout problem to an LBB type instability. In order to pursue this argument, the authors interpret the layout optimization problem as a mixed variational problem in the density variable ρ and the displacement field u. To avoid the formation of checkerboard patterns, the authors suggest that different functions be used to interpolate ρ and u, in a fashion similar to that suggested by the LBB condition in other mixed problems. Unfortunately, the conditions under which the standard Babuska-Brezzi arguments are applied to mixed variational problems are not met by the layout optimization problem (Bendsøe 1994). If indeed a Babuska-Brezzi type, that is, a global kind of instability, were at work here a more complete analysis would be needed to formulate stability conditions appropriate for the layout optimization problem. Such an analysis is presented by Jog and Haber (1994).

In this paper, we suggest that checkerboard patterns in layout optimization can be explained on the basis of *local* behaviour. We will show that numerical approximations introduced by the finite element method may cause material arranged in a checkerboard fashion to appear *artificially* strong. When this happens checkerboard arrangements appear to be *locally* stronger than any other arrangement of two constituent materials, including a layered arrangement, and are a stable extremum of the strain energy density. Under such conditions checkerboard patterns are preferred in layout optimization problems seeking the stiffest structure.

2 The layout optimization problem

We will focus the discussion on two-dimensional elasticity problems, although some of the results presented here can be applied to plate and some three-dimensional elasticity problems as well. The optimization problem is standard: the goal is to minimize the mean compliance of the structure subject to a single constraint on the amount of available material. A distinguishing feature of current methods is the way the design variable at a point is related to the material properties.

Two strategies are common: one based on homogenization and another based on a variable thickness formulation. The homogenization based problem will be addressed first. Results specific to the variable thickness formulation will be summarized in the last section.

2.1 Layout optimization using homogenization

In this approach, shape is represented as a property of the "porous" material that results from the mixture of two (isotropic) constituents: a weak material, with the elasticity tensor E^- used to model a void, and a strong material with elasticity tensor $E^+ \gg E^-$. The proportion of strong material is measured by the scalar function $\rho : \Omega \to [0,1]$ where $\Omega \subset R^2$ is the domain where the structure is to be laid. The effective elastic properties of the mixture are obtained via homogenization assuming that the mixture occurs periodically and at a scale much smaller than the dimensions of Ω. Typically, the small scale mixture is characterized by a unit cell which in essentially all layout optimization applications is either a square cell with a rectangular hole (Fig. 2a), as introduced by Bendsøe and Kikuchi (1988), or a layered material (Fig. 2b), e.g. as discussed by Milton and Kohn (1988) and Milton (1990). In both cases, the amount of strong material is measured by the density function

$$\rho = a_1 + a_2 - a_1 * a_2 \,.$$

The effective property tensor $\overline{E}$ is expressed as a function of the parameters: a_1, a_2, E^-, E^+.

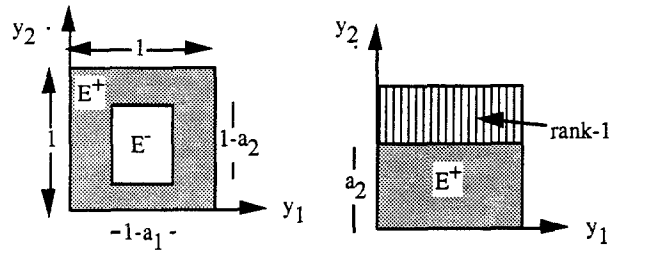

(a) Cell with rectangular hole (b) Rank 2 material

Fig. 2. Typical cell arrangements used in layout optimization

Design variables in the optimization problem are the spatial distribution of ρ and cell parameters $\{a_1, a_2\}$. As it is well-known that the optimum orientation of the material tensor can be obtained from the directions of principal strain (or stress) (Pedersen 1989), the orientation angle is not listed *explicitly* as an additional design variable. The goal is to minimize the mean compliance of the structure while keeping the amount of strong material bounded, i.e. to solve the problem

$$\min_{\rho \in X_R} \min_{a \in X_P} f(u^*), \tag{1}$$

where

$$X_R = \left\{ \rho \in L^\infty(\Omega) : \; 0 \le \rho \le 1, \; \int_\Omega \rho \, \mathrm{d}x \le R \right\} \tag{2a}$$

and

$$X_\rho = \left\{ a \in R^2 : \; a_1 + a_2 - a_1 * a_2 = \rho, \; 0 \le a_1 \le 1, \; 0 \le a_2 \le 1 \right\}. \tag{2b}$$

In (1), $f(u^*)$ is the mean compliance at the equilibrium solution u^* and R is a prescribed upper bound on the amount of available material. Problem (1) can be written in the equivalent form

$$\max_{\rho \in X_R} \min_{u \in K} \left\{ \int_\Omega \max_{a \in X_\rho} w \, \mathrm{d}x - f(u) \right\}, \tag{3}$$

where

$$K = \left\{ u^h \in H^1(\Omega) : \; u^h = 0 \text{ on } \Gamma^0 \right\}$$

represents the set of all kinematically admissible displacement fields u and

$$w = \frac{1}{2} \overline{E}(a) \varepsilon(u) : \varepsilon(u) \tag{4}$$

is the strain energy density associated with a given strain field $\varepsilon(u)$. Details of this derivation are well-known and may be found, for example, in the work of Lipton (1994) and Jog *et al.* (1992).

Statement (3) emphasizes the following well-known result: *for fixed density ρ and strain fields $\varepsilon(u)$, the optimum local orthotropy is such that the strain energy density is maximized.* This result is important in the determination of the stability of checkerboard solutions. The elasticity problem in (3) is typically solved using a finite element method and, as we shall show in what follows, some finite element approximations are such that arranging the material in a checkerboard fashion maximizes the strain energy. This is the main result in this paper, and is expressed as Proposition 1 in the next section.

2.2 Checkerboards and finite element discretization

To facilitate the analysis it is assumed that Ω can be covered by N *square* finite elements. Approximating u by u^h and ρ by ρ^h (3) becomes

$$\max_{\rho^h \in X_R^h} \min_{u^h \in K^h} \left\{ \sum_{e=1}^{N} \frac{1}{2} \int_e \max_{a^e \in X_{\rho^e}} \overline{E}(a^e) \varepsilon(u^e) \cdot \varepsilon(u^e) \, \mathrm{d}x - f(u^h) \right\}. \tag{5}$$

Standard finite element shape functions $N_\alpha(x)$ are used to construct $u^h \in K^h \subset K$ whose restrictions to element e are of the form

$$u^e = \sum_{\alpha=1}^{n} N_\alpha(x) u_\alpha^e, \quad n = \text{number of nodes},$$

where the u_α^e are nodal degrees of freedom. Regarding the discretization of the density ρ, here we limit the exposition to the more commonly used scheme and prescribe ρ^h to be constant within each element e, with value ρ^e.

The presentation is simplified by limiting the analysis to "black-and-white", i.e. strong-weak material checkerboard mixtures of *average* density 1/2. In a typical patch P of elements labeled 1 through 4 a "black-and-white" checkerboard distribution is $\{\rho^1, \rho^2, \rho^3, \rho^4\} = \{0,1,0,1\}$. We shall compare the stiffness of P with the effective stiffness of a mixture that uses the same amount of strong material, that is, a homogenized material with $\rho = 1/2$. The stiffness of "grey" patches is not discussed here, but numerical experiments have shown that results presented for purely black-white patches carry through for patches of elements of intermediate densities.

The main result of this paper states that some finite element discretizations make checkerboard patches appear to be artificially efficient. This result is summarized in Proposition 1 below.

Proposition 1. For all nonzero strain fields $\bar{\varepsilon}$
(i) in meshes of four-node elements

$$w^{CH}_{4\text{Node}}(\bar{\varepsilon}) \equiv \frac{1}{2}\overline{E}^{CH}_{4\text{Node}}\bar{\varepsilon}\cdot\bar{\varepsilon} \geq \frac{1}{2}\max_{\substack{a^e\in X_{\rho^e}\\ \rho^e=\frac{1}{2}}} \overline{E}(a^e)\bar{\varepsilon}\cdot\bar{\varepsilon}\,, \tag{6a}$$

(ii) in meshes of nine-node elements

$$w^{CH}_{9\text{Node}}(\bar{\varepsilon}) \equiv \frac{1}{2}\overline{E}^{CH}_{9\text{Node}}\bar{\varepsilon}\cdot\bar{\varepsilon} < \frac{1}{2}\max_{\substack{a^e\in X_{\rho^e}\\ \rho^e=\frac{1}{2}}} \overline{E}(a^e)\bar{\varepsilon}\cdot\bar{\varepsilon}\,. \tag{6b}$$

The functions $w^{CH}_{4\text{Node}}$ and $w^{CH}_{9\text{Node}}$ measure the strain energy density in a material with elasticity tensors $\overline{E}^{CH}_{4\text{Node}}$ and $\overline{E}^{CH}_{9\text{Node}}$, respectively. These are the effective properties of a checkerboard arrangement that is kinematically *constrained* to deform in a fashion consistent with the corresponding finite element. This constraint results in a numerically induced, artificially high stiffness [without this constraint the *actual* stiffness of a microscale checkerboard is zero due to the stress singularities at the corners of the solid regions, as discussed by Berlyand and Kozlov (1992)]. If four-node elements are used, (6a) in Proposition 1 states that, at least asymptotically, a checkerboard arrangement with such constraint is *more* rigid than a layered microstructure that uses the same amount of strong material. In contrast, (6b) states that the kinematic constraint associated with 9-node elements does not stiffen the material as much and checkerboard arrangements are *less* rigid than a layered microstructure. We believe that this is sufficient to explain the formation of checkerboards in layout optimization problems. A "black-and-white" checkerboard patch subjected to a constant strain field will have the same strain energy as a four- element patch of material with stiffness tensor $\overline{E}^{CH}_{4\text{Node}}$ or $\overline{E}^{CH}_{9\text{Node}}$. Furthermore, upon refinement, the *numerical* behaviour of patches of finite elements will approach the behaviour of a material with effective properties $\overline{E}^{CH}_{4\text{Node}}$ or $\overline{E}^{CH}_{9\text{Node}}$. Due to numerical modeling checkerboard arrangements of four-node elements will *appear* to be more rigid than other arrangements using the same amount of resources and hence they will be preferred, i.e. they will be solutions of the inner problem in (5) over the four elements that make up P.

In order to verify the validity of Proposition 1 we need first to calculate the *effective properties* of a checkerboard $\overline{E}^{CH}_{4\text{Node}}$ and $\overline{E}^{CH}_{9\text{Node}}$. This will be discussed in the next section.

3 Effective properties of a checkerboard

Here we compute the elastic properties of a checkerboard arrangement of material in a unit cell Y divided in four equal, nonoverlapping quadrants Y^i such that $E = E^-$ in $Y^1 \cup Y^3$ and $E = E^+$ in $Y^2 \cup Y^4$. In contrast to standard applications of homogenization, where the goal is to estimate the properties of a composite (e.g. Berlyand and Kozlov 1992; Guedes and Kikuchi 1992), we seek instead to estimate the *asymptotic* behaviour of checkerboard patches of *finite elements*. Such properties can be obtained using the well-known formulae (for details, see Bensoussan *et al.* 1978)

$$\overline{E}_{ijk\ell} = \int_Y \{E_{ijk\ell} - E_{ijpq}\varepsilon^*_{pq}[\chi^{(k\ell)}]\}\,\mathrm{d}y\,, \tag{7}$$

using Y-periodic fields $\chi^{(k\ell)}_p$ *restricted to finite element spaces of interest* and discretizing the cell Y using only one element per quadrant Y^i. Strains $\varepsilon^*_{pq}[\chi^{(k\ell)}]$ may vary within the cell and are induced by the inhomogeneity of the material. The fields $\chi^{(k\ell)}_p \in V^h$ are Y-periodic, *finite element solutions* of the cell problem

$$\int_Y E_{ijpq}\{\varepsilon^*_{pq}[\chi^{(k\ell)}] - \varepsilon^{0(k\ell)}_{pq}\}\frac{\partial \nu_i}{\partial y_j}\,\mathrm{d}y = 0\,,$$

$$\text{for all } \nu \in V^h\,, \quad \text{and } k,\ell = 1,2\,. \tag{8}$$

The asymptotic stiffness properties of a *finite element patch* are obtained simply by building the finite element space V^h using the same shape functions used to approximate the average displacement field $u(x)$, i.e. by defining

$$V^h = \{\nu(y) \in R^2 :\ \nu(y) = N_\alpha(y)\nu^i_\alpha\,,\ \text{if } y \in Y^i\,,\ i = 1,\ldots,4\}\,,$$

where the nodal quantities ν^i_α are such that $\nu(0,y_2) = \nu(1,y_2)$ *and* $\nu(y_1,0) = \nu(y_1,1)$. All entries in the tensor of effective properties can be obtained from (7) after solving (8) using *three* uniform, unit pre-strains $\varepsilon^{0(k\ell)}_{pq}$, as discussed by Sigmund (1993).

3.1 Checkerboards of four-node elements

Four-node isoparametric elements with bilinear shape functions $N_\alpha(x)$ are the most commonly used elements in layout optimization. The solution of the cell problem (8) is particularly simple in this case and is such that

$$\varepsilon^*[\chi^{(k\ell)}] = 0\,. \tag{9}$$

In other words, the (periodic) deformation of a checkerboard patch of any number of four-node elements subject to a constant prestrain $\bar{\varepsilon}^{(k\ell)}$ is such that the strain in the patch is constant. For illustration the field χ corresponding to a prestrain $\bar{\varepsilon}_{11} = \bar{\varepsilon}_{22} = 1$ and $\bar{\varepsilon}_{12} = 0$ is illustrated in Fig. 3. From (9) and (7) it follows that the effective properties of the patch are simply the *arithmetic* average of E^+ and E^-. As $E^- = 0$,

$$\overline{E}^{CH}_{4\text{Node}} = \frac{1}{2}E^+\,.$$

This accounts for the high stiffness of patches of four-node elements and makes material distributions in checkerboard fashion particularly attractive. For example, if

$$E^- = 0,\ E^+_{1111} = E^+_{2222} = 1,\ E^+_{1122} = 0.3,\ E^+_{1212} = 0.35\,, \tag{10}$$

the effective properties are

$$\overline{E}_{1111} = \overline{E}_{2222} = 0.5,\ \overline{E}_{1122} = 0.15,\ \overline{E}_{1212} = 0.175\,.$$

3.2 *Checkerboards of nine-node elements*

Meshes of nine-node elements have many more displacement degrees of freedom per material design variable ρ^e than four-node element meshes. For this reason nine-node elements are seldom used in layout optimization, in spite of the fact that most authors report that solutions based on these elements have no checkerboards.

The solution of the cell problem (8) is qualitatively different from that of a four-node element patch. The inhomogeneities in the material result in a nonzero local strain variation, as illustrated in Fig. 3b. For this reason, patches of nine-node elements are more flexible than their four-node counterparts. For example, with constitutive material as before (10), analytical solution of (7) and (8) yields

$$\overline{E}_{1111} = \overline{E}_{2222} = 0.172,\ \overline{E}_{1122} = 0.0941,\ \overline{E}_{1212} = 0.1159\,.$$

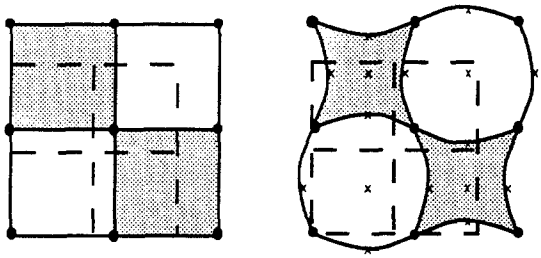

(a) 4-node elements (b) 9-node elements

Fig. 3. Local field χ due to a mean strain $\bar{\varepsilon}_{11} = \bar{\varepsilon}_{22} = 1$ and $\bar{\varepsilon}_{12} = 0$

4 Local optimality of checkerboard material distributions

4.1 *Problem using layered materials*

We now can prove Proposition 1. Consider first the layout optimization problem using layered materials (Fig. 2a). For fixed strains and density $\rho = 1/2$, let w^*_{Rank2} be the optimum strain energy density, i.e.

$$w^*_{\text{Rank2}} = \frac{1}{2} \max_{\substack{a^e \in X \\ \rho^e = \frac{1}{2}}} \overline{E}_{R2}(a)\varepsilon \cdot \varepsilon\,. \tag{11}$$

In (11) a_1 and a_2 are layer thicknesses and $\overline{E}_{R2}$ is the tensor of the effective properties of a rank 2 material. If the weak material is *void* ($E^- = 0$) it is possible to express w^*_{Rank2} explicitly using the results from the paper by Jog *et al.* (1992), as follows:

$$\frac{w^*_{\text{Rank2}}}{E^+_{1111}\varepsilon_I^2} =$$

$$\begin{cases} \dfrac{[1+\eta(1-\nu)+\eta^2](1+\nu)}{3+\eta} & \text{if} \quad \eta < -\dfrac{(1+\nu)}{2} \\ \dfrac{[1+\eta(1-\nu)+\eta^2](1+\nu)}{3-\eta} & \text{if} \quad \eta > \dfrac{(1-\nu)}{2} \\ \frac{1}{4}(1-\nu^2) & \text{if} \quad -\dfrac{(1+\nu)}{2} < \eta < \dfrac{(1-\nu)}{2} \end{cases} \tag{12}$$

In (12) ν is the Poisson's ratio of the strong material, the material coordinate system is aligned with the directions of principal strain, $\eta = (\varepsilon_I/\varepsilon_{II})$ is the principal strain ratio and, by convention, $|\varepsilon_I| > |\varepsilon_{II}|$.

Consider now the strain energy density in a material with the effective properties of a checkerboard [obtained by solving (7) and (8)].

(a) Made of four-node elements. The strain energy density is

$$\frac{w^*_{\text{4Node}}}{E^+_{1111}\varepsilon_I^2} = \frac{1}{4}(1 + 2\nu\eta + \eta^2)\,. \tag{13}$$

(b) Made of nine-node elements. The strain energy density is

$$\frac{w^*_{\text{9Node}}}{E^+_{1111}\varepsilon_I^2} =$$

$$\frac{1}{4}\left[\frac{(47 - 35\nu - 35\nu^2 + 25\nu^3)}{22(6-5\nu)} + \right.$$

$$\frac{(50 - 26\nu - 70\nu^2 + 50\nu^3)}{22(6-5\nu)}\eta +$$

$$\left.\frac{(47 - 35\nu - 35\nu^2 + 25\nu^3)}{22(6-5\nu)}\eta^2\right] \tag{14}$$

It can be easily verified that for any strain ratio η

$$w^*_{\text{4Node}} \geq w^*_{\text{Rank2}} \quad \text{and} \quad w^*_{\text{9Node}} < w^*_{\text{Rank2}}\,, \tag{15}$$

and $w^*_{\text{4Node}} = w^*_{\text{Rank2}}$ only for $\eta = -\nu$. These energies are plotted in Fig. 4 for $\nu = 0.3$. This proves Proposition 1 for a layered material.

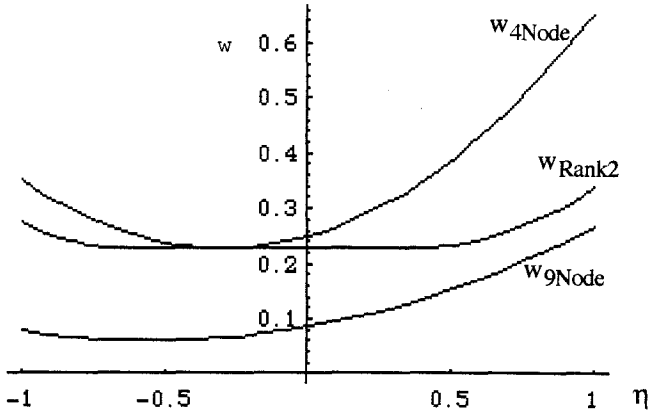

Fig. 4. Strain energy density of a layered material compared to numerical behaviour of checkerboards

4.2 *Problem using a rectangular hole cell*

The results of the previous section remain essentially unchanged if the small scale mixture is characterized by a square cell with a rectangular hole (Fig. 2a). From the optimality of layered materials (Avellaneda 1987) it is known that

$$w^*_{R2} \geq w^*_{R\text{Hole}} = \frac{1}{2} \max_{\substack{a^e \in X_{\rho^e} \\ \rho^e = \frac{1}{2}}} \overline{E}_{R\text{Hole}}(a)\varepsilon \cdot \varepsilon\,,$$

and therefore it follows from (15) that $w^*_{\text{4Node}} \geq w^*_{R\text{Hole}}$. The derivation of the result for nine-node elements is only slightly more complicated in this case as an explicit expression for the optimal energy such as (14) is not available. A numerical calculation for a material as before (10) yields the results shown in Fig. 5. As before,

$$w^*_{\text{4Node}} > w^*_{R\text{Hole}} > w^*_{\text{9Node}}\,.$$

Therefore, in this case too the checkerboard arrangement of material is optimal for four- and *not* for nine-node element checkerboards.

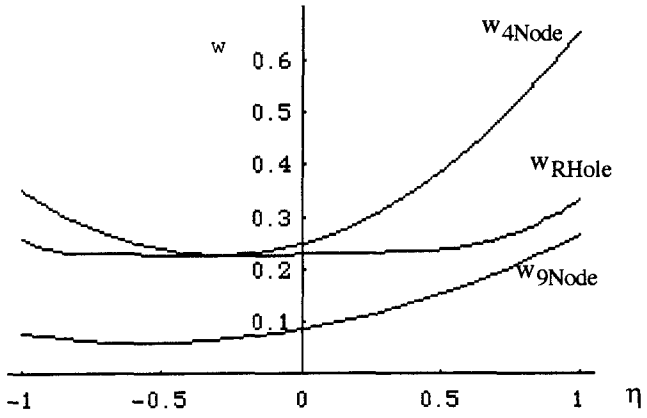

Fig. 5. Strain energy density of a suboptimal microstructure compared to numerical behaviour of checkerboards

4.3 Problem using a modified variable thickness formulation

A popular layout optimization strategy that is not based on a homogenization procedure uses the simple rule

$$\overline{E}(\rho) = \rho^p E^+ \quad \text{with} \quad p > 0\,. \tag{16}$$

This approach, labeled here the *variable thickness formulation*, has been used by several authors (e.g. Mlejnek and Schirrmacher 1993) to solve layout optimization problems of the form [c.t. (5)]

$$\max_{\rho^h \in X_R^h} \min_{u^h \in K^h} \sum_{e=1}^{N} \frac{1}{2} \int_e (\rho^e)^p E^+ \varepsilon(u^e) \cdot \varepsilon(u^e)\, \mathrm{d}x - f(u^h)\,,$$

with the feasible set

$$X_R = \left\{ \rho \in L^\infty(\Omega) :\ 0 \le \rho \le 1,\ \int_\Omega \rho\, \mathrm{d}x \le R \right\}.$$

The strain energy density is

$$w^*_{V\mathrm{Thick}} = \frac{1}{2} \left(\frac{1}{2}\right)^p E^+ \bar{\varepsilon} \cdot \bar{\varepsilon}$$

at a point where the strain is $\bar{\varepsilon}$ and the density of strong material is $\rho = 1/2$, the effective density of a "black-and-white" checkerboard. In terms of the principal strains

$$\frac{w^*_{V\mathrm{Thick}}}{E^+_{1111}\varepsilon_I^2} = \frac{1}{2}\left(\frac{1}{2}\right)^p (1 + 2\nu\eta + \eta^2)\,.$$

Hence, from (13), for a material with $p = 1$ the strain energy density $w^*_{V\mathrm{Thick}}$ is the same as the energy density in a checkerboard made of four-node elements. For $p = 1$ and *higher*

$$w^*_{4\mathrm{Node}} \ge w^*_{V\mathrm{Thick}}, \quad p \ge 1\,,$$

and hence checkerboards are also expected here if fine meshes are used. A similar result can be derived for meshes of nine-node elements. This is summarized in Proposition 2 below.

Proposition 2. For all nonzero strain fields $\bar{\varepsilon}$,
(i) in meshes of four-node elements

$$w^*_{4\mathrm{Node}}(\bar{\varepsilon}) = w^*_{V\mathrm{Thick}}(\bar{\varepsilon}), \quad \text{for } p = 1\,,$$

and

$$w^*_{4\mathrm{Node}}(\bar{\varepsilon}) > w^*_{V\mathrm{Thick}}(\bar{\varepsilon}), \quad \text{for } p > 1\,,$$

(ii) in meshes of nine-node elements

$$w^*_{9\mathrm{Node}}(\bar{\varepsilon}) < w^*_{V\mathrm{Thick}}(\bar{\varepsilon}), \quad \text{for } p < p_1^*(\nu)\,,$$

and

$$w^*_{9\mathrm{Node}}(\bar{\varepsilon}) > w^*_{V\mathrm{Thick}}(\bar{\varepsilon}), \quad \text{for } p > p_2^*(\nu)\,,$$

where

$$p_1^*(\nu) = \frac{\log[22/(6-5\nu)]}{\log(2)}, \quad p_2^*(\nu) = \frac{\log[2\cdot(6-5\nu)]}{\log(2)}\,.$$

Figure 6 shows the variation of p^* with Poisson's ratio while Fig. 7 shows the variation of $w^*_{V\mathrm{Thick}}$ with strain for different values of p. Proposition 2 suggests that for larger values of p checkerboards will appear even in problems where nine-node elements are used. The analysis also indicates that contrary to conventional wisdom, checkerboards are possible in the standard variable thickness sheet problem in optimization, which corresponds to $p = 1$. Numerical experiments support these findings. They also show that "grey" checkerboard patterns of average density *below* 1/2 can occur for *any* p greater than 1.

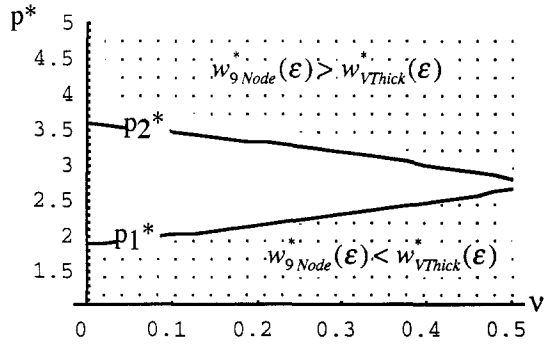

Fig. 6. Variation of p^* with Poisson's ratio of the strong material

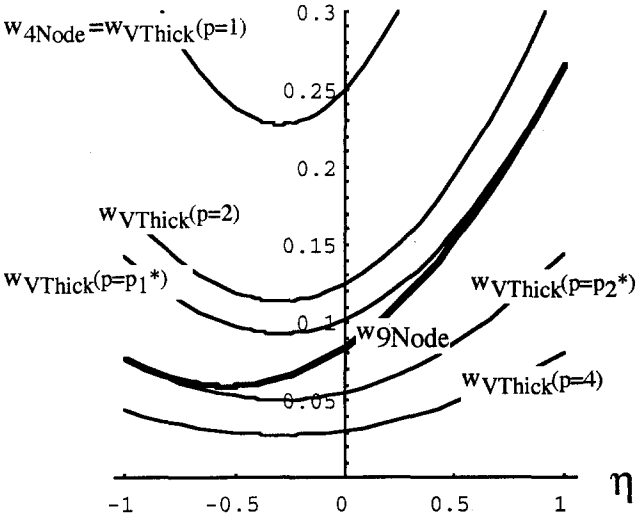

Fig. 7. Strain energy density in variable thickness formulations ($\nu = 0.3$)

5 Conclusions

We have computed the *numerical* behaviour of arrangements of strong and weak materials in a checkerboard fashion where

the deformation is constrained to be typical of a finite element space (bilinear for four-node elements, biquadratic for nine-node elements). The numerical asymptotic behaviour of four-node element patches has been shown to be artificially stiff, indeed stiffer than any "real" material built, for example, by layering two isotropic constituents. This artificially high stiffness can account for the formation of checkerboard patterns in continuous layout optimization problems of compliance minimization. We should emphasize that this analysis was limited to black-white checkerboards, i.e. effective densities equal to 1/2. The limits of stability of solutions are likely to be different when other effective densities are considered. Nevertheless, it is expected that the *mechanism* whereby checkerboards are formed remains the same. This is indeed supported by numerical experiments.

Acknowledgements

This research was supported, in part, by grant DDM-9201882 (AD and OS) from the National Science Foundation and the Danish Technical Research Council through the Program on Computer Aided Design (OS). This support is gratefully acknowledged.

References

Avellaneda, M. 1987: Optimal bounds and microgeometries for elastic two-phase composites. *SIAM J. Appl. Math.* **47**, 1216-1228

Bendsøe, M.P. 1989: Optimal shape design as a material distribution problem. *Struct. Optim.* **1**, 193-202

Bendsøe, M.P. 1994: *Methods for the optimization of structural topology, shape and material.* Berlin, Heidelberg, New York: Springer (to appear)

Bendsøe, M.P.; Díaz, A.; Kikuchi, N. 1992: Topology and generalized layout optimization of elastic structures. In: Bendsøe, M.P. and Mota Soares, C.A. (eds.), *Topology design of structures*, pp. 159-205. Dordrecht: Kluwer

Bendsøe, M.P.; Kikuchi, N. 1988: Generating optimal topologies in structural design using a homogenization method. *Comput. Meth. Appl. Mech. Engrg.* **71**, 197-224

Bensoussan, A.; Lions, J.-L.; Papanicolaou, G. 1978: *Asymptotic analysis for periodic structures.* Amsterdam: North-Holland

Berlyand, L.V.; Kozlov, S.M. 1992: Asymptotics of homogenized moduli for the elastic chess-board composite. *Arch. Rational Mech. Anal.* **118**, 95-112

Brezzi, F.; Fortin, M. 1991: *Mixed and hybrid finite element methods.* Berlin, Heidelberg, New York: Springer

Guedes, J.; Kikuchi, N. 1992: Pre- and postprocessing for materials based on the homogenization method with adaptive finite elements. *Comp. Meth. Appl. Mech. & Engng.* **83**, 143-198

Jog, C.S.; Haber, R.B. 1994: Stability of finite element models for distributed-parameter optimization and topology design. *TAM Report No. 758.* Theoretical and Applied Mechanics, University of Illinois at Urbana-Champaign

Jog, C.S.; Haber, R.B.; Bendsøe, M.P. 1992: Topology design using a material with self-optimizing microstructure. In: Bendsøe, M.P.; Mota Soares, C.A. (eds.) *Topology design of structures*, pp. 219-238. Dordrecht: Kluwer

Lipton, R. 1994: On the relaxation for optimal structural compliance. *JOTA* **81**, 549-568

Mlejnek, H.P.; Schirrmacher, R. 1993: An engineering approach to optimal material distribution and shape finding. *Comp. Meth. Appl. Mech. & Engng.* **106**, 1-26

Milton, G. 1990: On characterizing the set of possible effective tensors of composites: the variational method and the translation method. *Comm. Pure Appl. Math.* **43**, 63-125

Milton, G.; Kohn, R.V. 1988: Variational bounds on the effective moduli of anisotropic composites. *J. Mech. Phys. Solids* **36**, 597-629

Pedersen, P. 1989: On optimal orientation of orthotropic materials. *Struct. Optim.* **1**, 101-106

Sigmund, O. 1994 : Materials with prescribed constitutive parameters: an inverse homogenization problem. *Int. J. Solids Struct.* **31**, 2313-2329

Received Dec. 14, 1994